ISTITUTO NAZIONALE DI FISICA NUCLEARE

Sezione di Genova

INFN/BE-94/04
26 Ottobre 1994

G. Testera, G. Drago, V. Lagomarsino, G. Manuzio:

DETECTION OF HIGH ENERGY PARTICLES STORED IN A PENNING TRAP

Servizio Documentazione
dei Laboratori Nazionali di Frascati

INFN - Istituto Nazionale di Fisica Nucleare
Sezione di Genova

INFN/BE-94/04
26 Ottobre 1994

DETECTION OF HIGH ENERGY PARTICLES STORED IN A PENNING TRAP

G. Testera[2], G. Drago[1], V. Lagomarsino[2], G. Manuzio[2]

1) Department of Electrical Engineering, University of Genoa
2) Department of Physics, University of Genoa; National Institute of Nuclear Physics, Genoa

ABSTRACT

This article presents the results of our work about the signal induced on the electrodes of a Penning trap by oscillating particles with an amplitude which is comparable with the trap dimensions (that is to say with energy of the order of magnitude of the potential well which permits the confinement in the trap). The detection sensibility is calculated whether for radial motion or for the axial motion as a function of the particle energy and radial position. Quantitative analysis of the results shows a notable non linearity between the detected signals and the oscillation amplitudes.

1. Introduction

Penning traps are widely used to measure fundamental properties of the stored particles (such as masses and magnetic momenta) with very high precision [1],[2]. Every measurement of this kind can be reduced to a measure of some frequency of the stored particle motion and frequency resolution of the order of 10^8 or better can be obtained by a careful control of every disturbance which can alter the ideal motion inside the trap. In order to minimize the effects coming from mechanical imperfections, electrodes truncation, magnetic field inhomogeneity and so on, the stored particles are usually detected only when they have very small oscillation amplitude compared with the trap dimensions. The detected electric signal, coming from the displacement of the induced charges on the trap electrodes, is then linearly related to the particle velocity as described in [3].

Recently the Penning traps have found a wide application as devices catching beams of particles in flight [4]. The energy of the captured particles is now of the same order of the potential well of the trap and therefore the particles oscillate inside the trap with amplitudes comparable with the trap dimensions. In this situation the induced signal cannot be calculated using the previous small oscillations approximation leading to the results of [3].

In this paper we analize, in a general way, both the signal coming from the axial and

the radial motion of the particles stored inside the trap and results were obtained which hold for every oscillation amplitude. The detection of particles stored inside the trap with high energy and big radii could be useful in order to obtain information about the mean energy and the mean radial position of the stored bunch and to obtain the pick-up signal for the stochastic cooling process [5], [6]. The requested precision is several orders of magnitude less than that which is necessary to perform the measurements described in [1] and [2].

We first recall some general result about the motion of particles stored in an ideal Penning trap and about the induced currents on a conductor by moving charges. Finally we show the results about the calculated signal for the axial and radial motion of particles stored in Penning traps having different dimensions.

2. Penning traps

A Penning trap [1] is a particular trap for charged particles having the electrodes shaped as revolution hyperbola. Fig. 1 shows an axial section of this trap. When a voltage V_0 is applied between the ring and the two cups the electrostatic potential generated inside the trap is

$$V(r,z) = \frac{-V_0}{r_0^2 + 2z_0^2} \ (r^2 - 2z^2) \qquad (1)$$

A particle, whose charge is q, if $qV_>0$ feels a harmonic electric field along the z direction leading to

$$z(t) = A_z \cos(\omega_z t + \phi_z) \tag{2}$$

where

$$\omega_z = \sqrt{\frac{4qV_0}{m(r_0^2 + 2z_0^2)}} \tag{3}$$

and m is the particle mass. The amplitude A_z and the phase ϕ_z are related to the initial conditions.

Because the radial electric field is defocusing, to obtain a stable orbit it is necessary to place the trap inside a proper uniform magnetic field B directed along the z axis. The radial motion is then completely decoupled from the axial one and can be described by

$$x(t) + iy(t) = r_m \exp i(\omega_m t + \phi_m) + r_c \exp i(\omega_c t + \phi_c) \tag{4}$$

where the cyclotron angular velocity ω_c is

$$\omega_c = \frac{1}{2}\left[\frac{qB}{m} + \sqrt{\left(\frac{qB}{m}\right)^2 - 2\omega_z^2}\right] \tag{5}$$

and the magnetron angular velocity ω_m is

$$\omega_m = \frac{1}{2}\left[\frac{qB}{m} - \sqrt{\left(\frac{qB}{m}\right)^2 - 2\omega_z^2}\right] \tag{6}$$

The cyclotron radius r_c, the magnetron radius r_m and the phases ϕ_m and ϕ_c can be calculated knowing the initial position and velocity of the particle.

Normally

$$\omega_m << \omega_z << \omega_c$$

and so the energy of the stored particle is related principally to the amplitude of the axial motion and of the cyclotron motion. The magnetron radius characterizes the mean radial position of the particle internally within the trap.

3. Induced currents on the trap electrodes

The motion of a stored particle inside the trap produces a displacement of induced charges on the trap electrodes that is a current through a circuit connected between any trap electrode E and ground. The current $i_E(t)$ is obviously related to the induced charge $Q_E(t)$ by

$$i_E(t) = \frac{dQ_E(t)}{dt} \tag{7}$$

When the potential of the electrodes are held constant, it is possible to compute the charge $Q_E(t)$ generated by a particle in the position $x(t), y(t), z(t)$ using the simple relation [7]

$$Q_E(t) = -qU_E(x(t), y(t), z(t)) \tag{8}$$

The function U_E must be calculated solving the Laplace equation

$$\nabla^2 U_E = 0 \tag{9}$$

satisfying the boundary conditions

$$U_E = 1 \ \ on \ \ the \ \ electrode \ \ E$$

$$U_E = 0 \ \ on \ \ the \ \ other \ \ electrodes \tag{10}$$

This is a general result coming from the Gauss identity.

From (7) and (8) it follows

$$i_E(t) = -q \ \ \vec{v}(t) \ \ \vec{\nabla} U_E((x(t), y(t), z(t)) \tag{11}$$

This last equation clearly shows how the induced current is related to the particle motion - described by the particle velocity $\vec{v}(t)$ - and to the geometry of the surrounding conductors which determines the function U_E.

When it is possible to assume that

$$\frac{A_z}{z_0}, \frac{r_m}{r_0}, \frac{r_c}{r_0} << 1 \tag{12}$$

the function giving the charge Q_{cup}, induced on the upper cup of the trap shown in figure 1, may be approximated in the following way

$$Q_{cup}(t) = -q\alpha_z \left(\frac{z}{2z_0} + \frac{1}{2} \right) \tag{13}$$

The constant coefficient α_z is a number < 1 depending upon the ratio r_0/z_0 as the calculations performed in [3] show.

The induced current is then linearly related to the axial oscillation amplitude

$$i_{cup}(t) = q\alpha_z \frac{A_z}{2z_0}\omega_z \sin(\omega_z t + \phi_z) \tag{14}$$

that is, provided that the amplitude is sufficiently small, for a given trap the "detection sensibility α_z" is not energy or position dependent. Note that, selecting $\alpha_z = 1$, equation (14) holds for every particle position inside a parallel plate capacitor having the plates at distance $2z_0$.

When condition (12) is satisfied a similar results holds for the charge Q_r induced on a ring sector

$$Q_r(t) = -q\alpha_r \left(\frac{x}{2r_0} + \frac{1}{2}\right) \tag{15}$$

The related current allows the radial motion detection

$$i_r(t) = q\alpha_r\omega_c \frac{r_c}{2r_0} \sin(\omega_c t + \phi_c) + q\alpha_r\omega_m \frac{r_m}{2r_0} \sin(\omega_m t + \phi_m) \tag{16}$$

α_r has a meaning equal to α_z but we cannot find any reliable publishied data.

In the usual detection network (figure 2a and 2b) the signals (14) and (16) act as input of resonant circuits tuned to the frequencies $\nu_z = \omega_z/(2\pi)$, $\nu_c = \omega_c/(2\pi)$ or $\nu_m = \omega_m/(2\pi)$ and connected to one cup for the monitoring of the axial motion and to a ring sector for the monitoring of the radial motion. This method normally allows the complete detection of protons, antiprotons or heavy ions and the detection af the magnetron and axial motion

of electrons. The cyclotron motion of electrons is normally in the microwave range and can be detected using different techniques [1].

4. Calculation of the U functions

As we anticipated in the introduction, we analized the signal coming from particles moving inside the trap with big oscillation amplitudes. When one consideres particles having large oscillation amplitudes two effects become important:

1) far from the center of a real trap the motion is no longer described by only three frequencies but anharmonicity effects could not be negligeable. This generally means that the ideal frequencies could be shifted and that the detected signal could have a large frequency spectrum centered around the new frequencies.

2) The induced charge $Q_E(t)$ must be calculated in the complete way solving the "equivalent electrostatic problem" described by equations (9) (10) and, even for an ideal trap having infinite electrodes, the problem can only be solved numerically.

In this paper we concentrated on point 2) and we calculated the induced signal from both the radial and the axial motion neglecting the anharmonicity effects in the particle motion.

The "equivalent electrostatic problem" which must be solved to determine U_{cup} can

be reduced, using cilindrical coordinates, to a two dimensional problem for the variable r, z. This simplification is not possible for the calculation of the U_s functions where s is a ring sector: in this case we must solve a 3D problem.

In both cases the charge distribution calculation was performed numerically using Finite Element Method. The two-dimensional axisimmetric problem was analyzed using $VF/PE2D$ electrostatic module solving a Laplace equation. The program uses a Galerkin weighted residual formulation for the finite element discretization of the differential equation and a Delaunay algorithm for the geometrical subdivision of the problem domain.

Instead the analysis of the 3D case was carried out using the VF/TOSCA [8] solver for the computation of the three-dimensional field and using the VF/OPERA enviroment to model the geometry. Even in this case the code is based on a standard Galerkin finite element scheme.

In order to allow an approximate evaluation of the accuracy of the calculations it can be mentioned that for the two dimensional cases a mesh of about 2200 nodes has been used (using first order triangular elements) while in the three dimensional analysis, with first order bricks elements, about 42.000 nodes have been employed.

5. Results about the axial motion

We studied Penning trap having different values for the ratio r_0/z_0 and we present results concerning traps with $r_0/z_0 = \sqrt{(2)}$, $r_0/z_0 = 1$, $r_0/z_0 = 0.6$. It is interesting to underline that traps with $z_0 > r_0$ are favorite for catching beam of particles in flight.

Fig. 3 shows the induced current on a cup of a trap having $r_0/z_0 = 0.6$ by a particle oscillating with $A_z/z_0 = 0.25$ and $r_m/r_0 = 0.5$, $r_c/r_0 = 0.1$ The picture shows that this current is a periodic function, having the same period as the particle axial velocity. It is important to evaluate the Fourier component with frequency ν_z because this is the only component of the signal that gives an output in the tuned detection system. To better compare the general signal to the signal coming from particle moving near the center of the trap we define $\alpha'_z(\frac{A_z}{z_0}, \frac{r_m}{r_0})$ in the following way

$$\alpha'_z = \sqrt{a_z^2 + b_z^2} \tag{17}$$

where

$$a_z = \frac{2}{T}\frac{2z_0}{\omega_z q A_z}\int_0^T i_{cup}(t)\cos\omega_z t)dt \tag{18}$$

$$b_z = \frac{2}{T}\frac{2z_0}{\omega_z q A_z}\int_0^T i_{cup}(t)\sin(\omega_z t)dt \tag{19}$$

T is a time interval longe enough to get results independent of the ϕ_z, ϕ_m and ϕ_c values.

Using (17) (18) (19) the current $i_{cup}(t)$ can be written

$$i_{cup}(t) = q \;\; \alpha'_z(\frac{A_z}{z_0}, \frac{r_m}{r_0}) \;\; \frac{A_z}{2z_0} \;\; \omega_z \;\; \sin(\omega_z t + \phi_z) \tag{20}$$

α'_z is equal to α_z for $r_m/r_0, A_z/z_0 << 1$ but, generally, is a function of r_m/r_0 and A_z/z_0. Looking at this function it is easy to see how signal (20) is different from the linear one described by (14) and how the detection sensibility is changing with the particle axial energy and mean radial position. Fig. 4a), 4b), 4c) show $\alpha'_z(A_z/z_0, r_m/r_0)$ versus A_z/z_0 keeping r_m/r_0 as parameter for three different Penning traps.

Fig. 4a,b,c indicates that while the amplitude is increasing the signal (20) rises faster than the linear one (14) but, for a given oscillation amplitude, the z motion is detected with a sensibility which decreases while the radius becomes bigger.

6. Results about the radial motion

We calculated the radial current i_{ring} detected in a circuit connected to one of the electrodes obtained by splitting, in the axial direction, the trap ring into four equal sectors (figure 2b). We are interested in the Fourier component with frequency ν_c and ν_m and we define $\alpha'_{c,m}$ using relations similar to (17), (18), (19)

$$\alpha'_{c,m} = \sqrt{a^2_{c,m} + b^2_{c,m}} \tag{21}$$

where

$$a_{c,m} = \frac{2}{T}\frac{2r_0}{\omega_{c,m} q r_{c,m}} \int_0^T i_{ring}(t) \cos(\omega_{c,m} t) dt \tag{22}$$

$$b_{c,m} = \frac{2}{T}\frac{2r_0}{\omega_{c,m} q r_{c,m}} \int_0^T i_{ring}(t) \sin(\omega_{c,m} t) dt \tag{23}$$

The results about the magnetron motion are simpler than the ones concerning the cyclotron motion because α'_m, as α'_z, depends only upon r_m/r_0 and A_z/z_0.

Fig. 5a, 5b, 5c shows the behaviour of α'_m.

The cyclotron motion detection sensibility α'_c is a more complicated function because it depends on A_z/z_0,r_m/r_0 and r_c/r_0 as fig. 6a, 6b, 7a, 7b, 8a, 8b show.

7. Observation about the signals with double frequency

For what concerns the axial motion it is very interesting to observe that it is possible to obtain a signal related to the axial oscillation amplitude but not depending on the radial particle position. This result can be achieved linking together the two cups of the trap and connecting them to a detection circuit tuned to $\nu'_z = 2\nu_z$. Equations (9) and (10) tell us that in this configuration the induced charge Q_{2cups} is

$$Q_{2cups} = q\left(\frac{r^2 - 2z^2}{r_0^2 + 2z_0^2} - \frac{2z_0^2}{r_0^2 + 2z_0^2}\right) \tag{24}$$

and taking into account equations (2) and (24) we easily obtain the induced current i_{2cups}

$$i_{2cups} = -q\frac{2A_z^2}{r_0^2+2z_0^2}\omega_z \sin 2(\omega_z t+\phi_z) - \frac{2q}{r_0^2+2z_0^2}xv_x - \frac{2q}{r_0^2+2z_0^2}yv_y \qquad (25)$$

This current has a Fourier component with frequency $2\omega_z$ which takes contribution mainly from the first addendum. Therefore, as we anticipated, the signal detected by the circuit tuned to $2\nu_z$ is practically independent on the radial particle position and it is proportional to the square of the axial oscillation amplitude.

A result similar to (25) holds for the current i_{2sect} flowing in a circuit tuned to $2\nu_c$ (or $2\nu_m$) and connected to two opposite radial ring sectors linked together

$$i_{2sect} = -\gamma q\frac{2r_m^2}{r_0^2+2z_0^2}\omega_m \sin 2(\omega_m t+\phi_m) + ... \qquad (26)$$

The γ coefficient has been evaluate numerically: it takes values near to 1 but, unfortunately, it is a function of the axial amplitude and of radial particle position very similar to α_c' (α_m'). Therefore for the radial motion also this new detection configuration do not allow to get a linear relation between the radial motion parameters and the measured signal.

7. Comments and conclusions

As expected, the results of our work show that generally in a Penning trap the relation between the particle oscillation amplitude and the electrical signal detected by a tuned circuit connected to the trap electrodes is not linear. Our calculations allow to specify this statement in a quantitative way at least for some typical configuration of the trap electrodes. In any case our results allow to establish some limit about the trap volume that the stored particles can occupy in order to get a signal which differs from the linear one of a given quantity.

Another results of our calculation concerns the informations that can be obtained measuring the induced signal coming from N particles stored inside the trap. The current I_z induced on one cup of the trap is obviously obtained summing the currents coming from every particle

$$I_z = \sum_{k=1}^{N} i_k(t) = q \;\; \omega_z \;\; \sum_{k=1}^{N} \alpha'_z\left(\frac{A_{zk}}{z_0}, \frac{r_{mk}}{r_0}\right) \;\; \frac{A_{zk}}{2z_0} \;\; \sin\left(\omega_z t + \phi_{zk}\right) \qquad (27)$$

It follows from this relation that the mean value of I_z^2 is directly proportional to the particle number times the quantity

$$< (\alpha'_z)^2 A_z^2 > \qquad (28)$$

that is

$$< I_z^2 >= \frac{q^2\omega_z^2}{8z_0^2} N < (\alpha_z')^2 A_z^2 > \tag{29}$$

When the particles oscillates near the trap center we can assume that the α_z' value is constant and in this situation measuring $< I_z^2 >$ we directly obtain the value of the product

$$N < A_z^2 > \tag{30}$$

In the general situation discussed in this article - when the oscillation amplitudes of the stored particles are not small compared with the trap dimensions - the value assumed by $< I_z^2 >$ is depending on the distribution of the axial oscillation amplitude and radii of the particles. Generally this distribution is unknown but, in any case, our calculations allow to make estimation of the possible errors about the evaluation of the mean axial oscillation amplitude (that is the mean axial energy) and particle number effettuated using different hypothesis for the distribution. The discussion can be extended in an easy way from the axial motion to the radial one. The axial motion present the advantage of allowing a good extimation of the product $N < A_z^2 >$ using the detection system described in section 6.

REFERENCES

[1] L. S. Brown, G. Gabrielse Rev. of Mod. Physics 58 n. 1 233 (1986)

[2] G. Gabrielse Phys. Rev. Lett. 65 n. 11 1317 (1990)

[3] G. Gabrielse Phys. Rev. A 29 462 (1984)

[4] J. Eades and others CERN PSSC 89-15 PSSC/P 118 (1990);

N. Beverini and others LOS ALAMOS report LA-UR-260 (1986)

[5] N. Beverini, V. Lagomarsino, G. Manuzio, F. Scuri, G. Testera, G. Torelli

Phys. Rev. A 38 n.2 107 (1988)

[6] V. Lagomarsino, G. Manuzio, G. Testera Phys. Rev. A 44 n.8 5173 (1991)

[7] E. Durand *Magnetostatique*, Masson and C^{ie} Editeurs (Paris 1968)

[8] C.S. Biddelcombe, C. P. Riley IEEE Trans. on Mag. 24 n.1 374 (1988)

FIGURES CAPTIONS

FIGURE 1

Axial section of a Penning trap.

FIGURE 2a

This figure shows the typical z motion detection network. The L_z and C_z values must satisfied the relation $\omega_z = \frac{1}{\sqrt{L_z C_z}}$

FIGURE 2b

This is a simple scheme to detect the radial motion. The two circuits are connected to two ring sectors; the upper is tuned to the cyclotron frequency and the lower to the magnetron frequency.

FIGURE 3

This figure shows the behaviour of $\frac{i_{cup}(t)}{q\omega_z}$ versus time (unif of $T_z = 2\pi/\omega_z$). Here i_{cup} is the current induced on a cup of a trap having $r_0/z_0 = 0.6$ by a particle oscillating with $A_z/z_0 = 0.25$, $r_m/r_0 = 0.5$, $r_c/r_0 = 0.1$ and $\omega_c/\omega_z = 6.61$,$\omega_m/\omega_z = 0.079$

FIGURES 4a,4b,4c

These figures show the values of the function $\alpha'_z(A_z/z_0, r_m/r_0)$ for Penning traps having $r_0/z_0 = \sqrt{(2)}$ $r_0/z_0 = 1$ and $r_0/z_0 = 0.6$. The α'_z values are plotted versus A_z/z_0; r_m/r_0 is the parameter which changes from curve to curve in the same plot. Going from the top curve to the bottom one r_m/r_0 takes the values $0; 1/10; 2/10; ....9/10$

FIGURES 5a,5b,5c

Values of $\alpha'_m(A_z/z_0, r_m/r_0)$ versus r_m/r_0 plotted using A_z/z_0 as parameter. Going from the top curve to the bottom one A_z/z_0 takes the values $0; 1/10; 2/10; ....9/10$.

Reading r_c/r_0 in place of r_m/r_0 these curves give the values of $\alpha'_c(\frac{A_z}{z_0}, \frac{r_m}{r_0} = 0, \frac{r_c}{r_0})$.

FIGURES 6a,6b; 7a, 7b; 8a,8b

Values of $\alpha'_c(\frac{A_z}{z_0}, \frac{r_m}{r_0}, \frac{r_c}{r_0})$ plotted versus $\frac{r_c+r_m}{r_0}$ keeping $r_m/r_0 = 0.2$ and $r_m/r_0 = 0.5$. To better compare these plots with fig. 5a,b,c the horizontal axis also shows the values of r_c/r_0 As usual the parameter describing the different curves is A_z/z_0 which keeps the same values as in fig. 5a,b,c. r_0/z_0 takes the value of $\sqrt{(2)}$, 1 and 0.6 going from fig. 6a and 6b to fig. 8a and 8b.

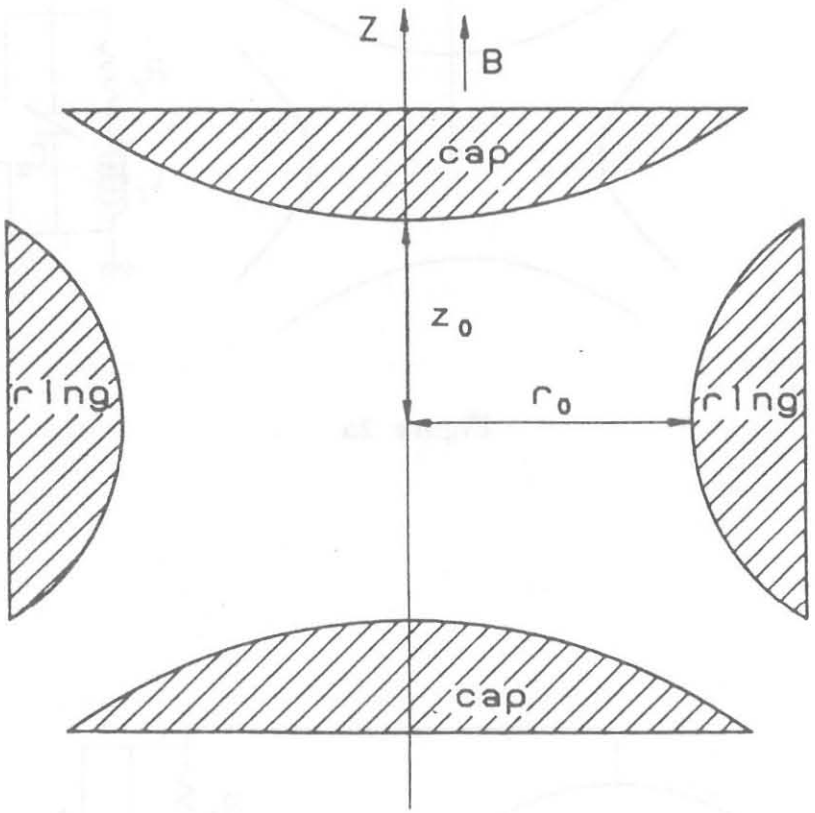

Figure 1

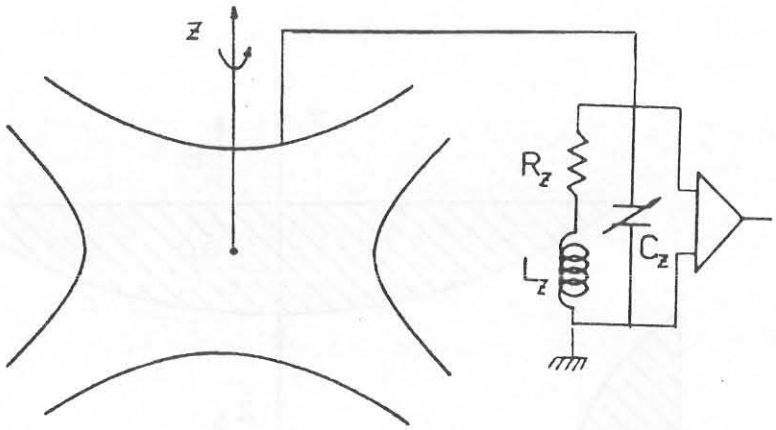

Figure 2a

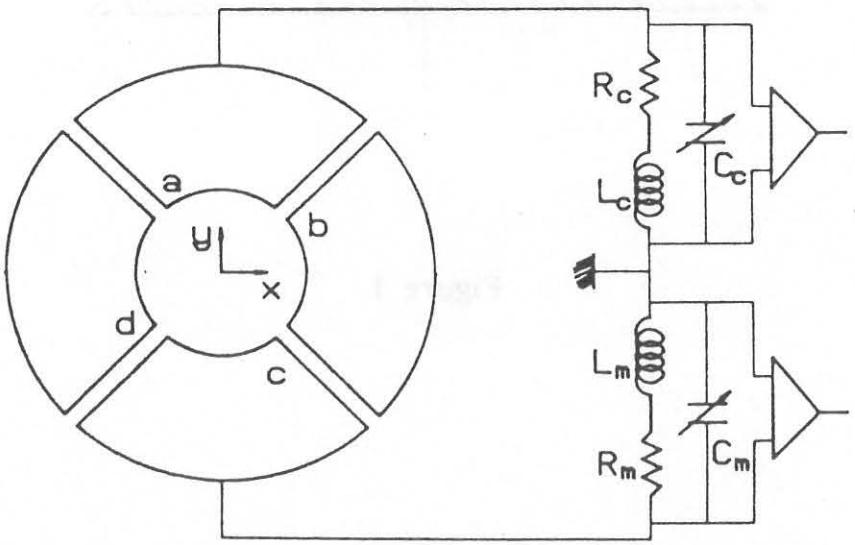

Figure 2b

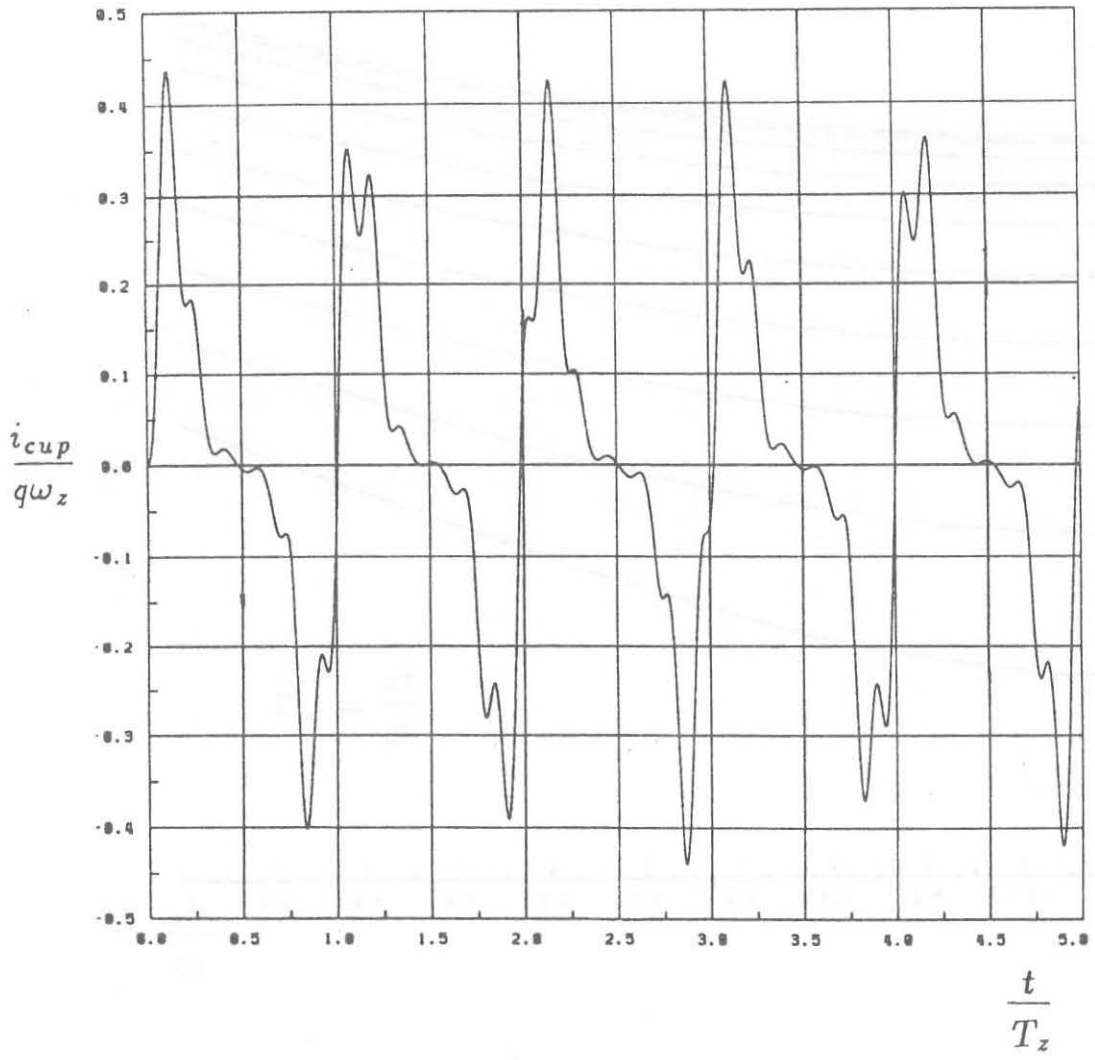
0.5
0.4
0.3
0.2
0.1
0.0
-0.1
-0.2
-0.3
-0.4
-0.5
0.0
0.5
1.0
1.5
2.0
2.5
3.0
3.5
4.0
4.5
5.0
$\frac{i_{cup}}{q\omega_z}$
$\frac{t}{T_z}$

Figure 3

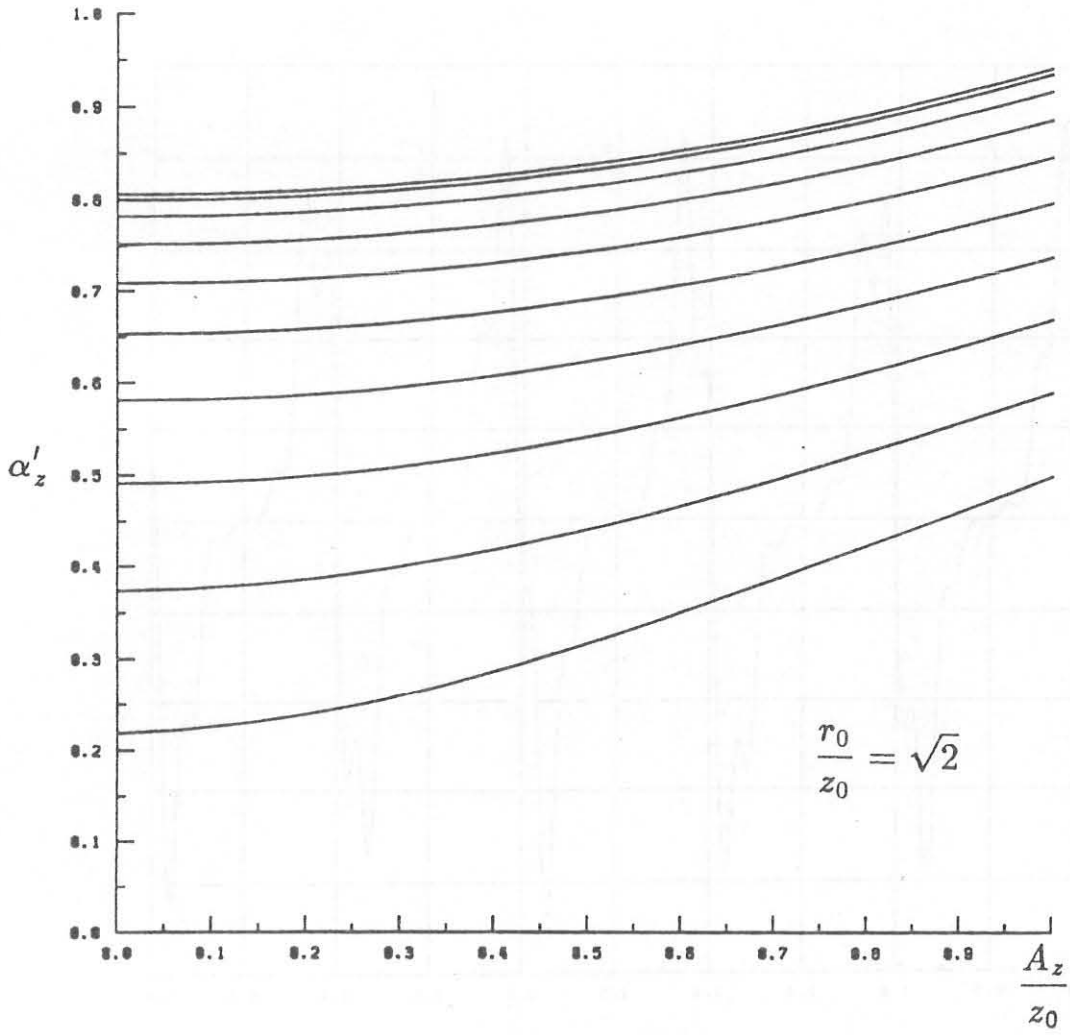
1.0
0.9
0.8
0.7
0.6
0.5
0.4
0.3
0.2
0.1
0.0
α'_z
0.0
0.1
0.2
0.3
0.4
0.5
0.6
0.7
0.8
0.9
$\frac{A_z}{z_0}$
$\frac{r_0}{z_0} = \sqrt{2}$

Figure 4a

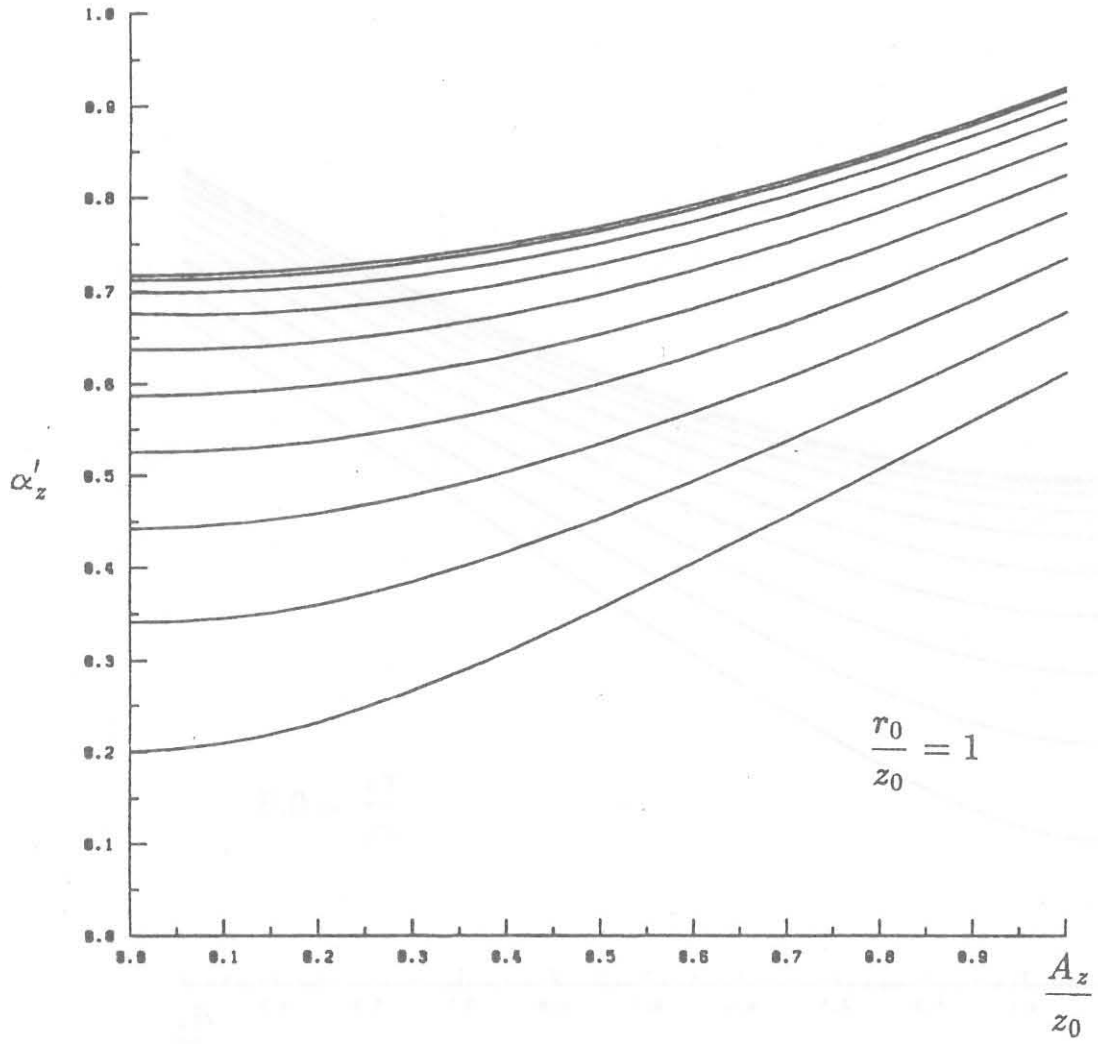
1.0
0.9
0.8
0.7
0.6
0.5
0.4
0.3
0.2
0.1
0.0
α'_z
$\frac{r_0}{z_0} = 1$
0.0
0.1
0.2
0.3
0.4
0.5
0.6
0.7
0.8
0.9
$\frac{A_z}{z_0}$

Figure 4b

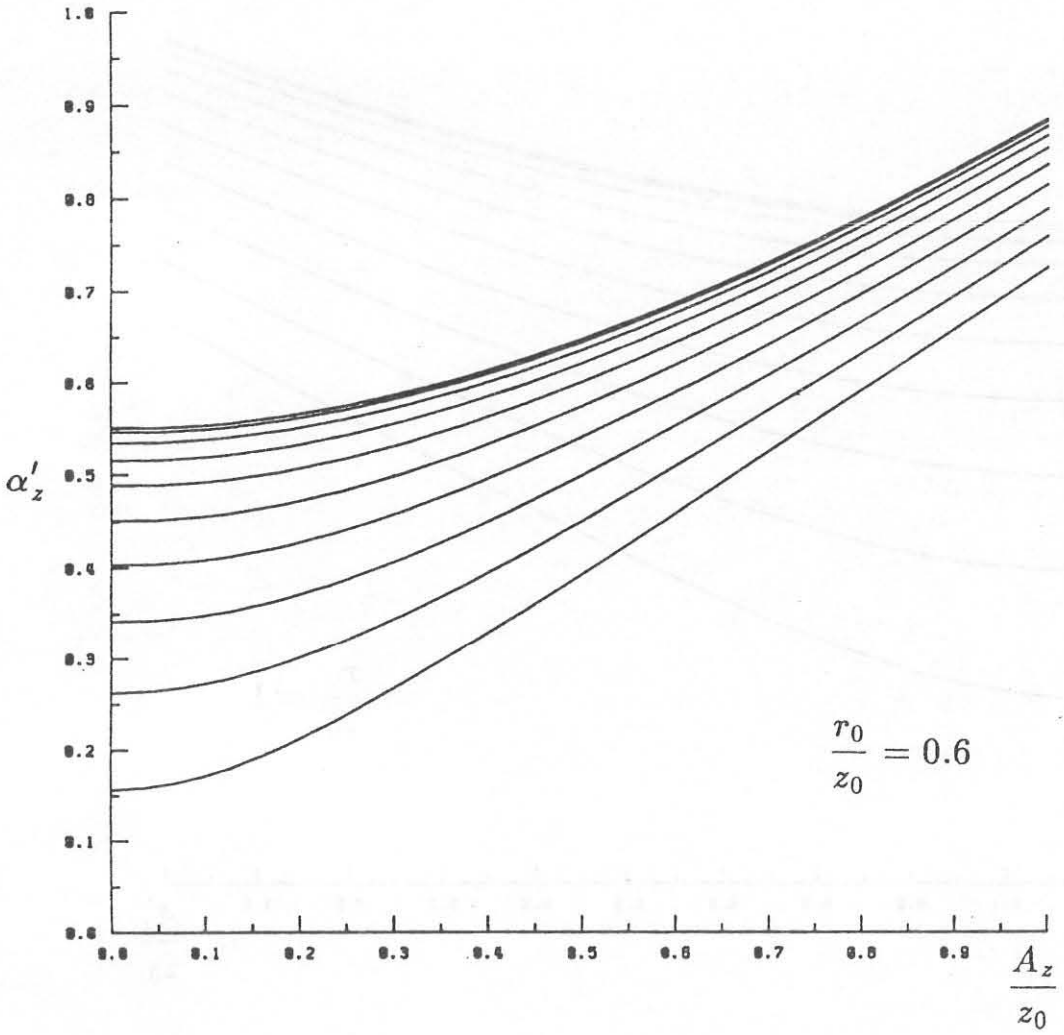
1.0
0.9
0.8
0.7
0.6
0.5
0.4
0.3
0.2
0.1
0.0
α'_z
0.0
0.1
0.2
0.3
0.4
0.5
0.6
0.7
0.8
0.9
$\frac{r_0}{z_0} = 0.6$
$\frac{A_z}{z_0}$

Figure 4c

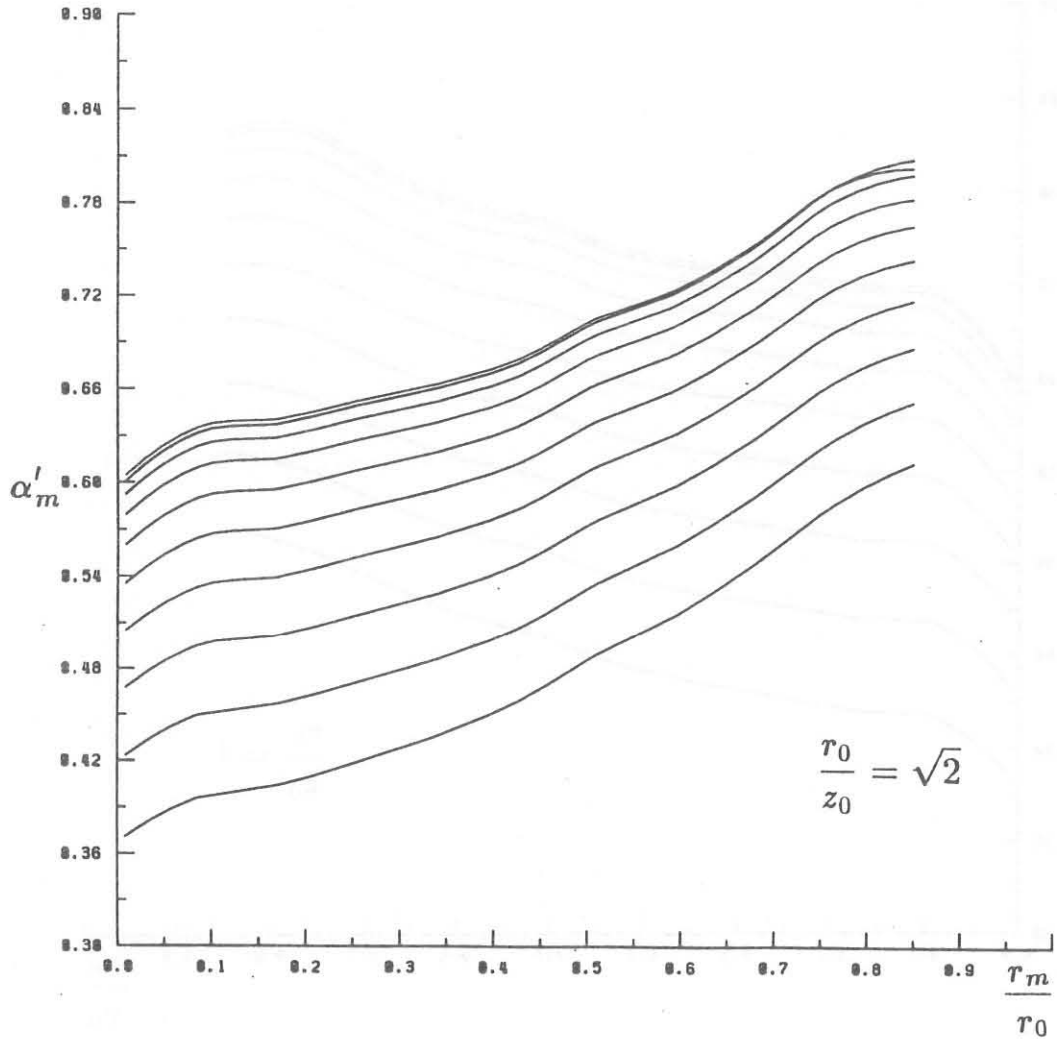
0.90
0.84
0.78
0.72
0.66
0.60
0.54
0.48
0.42
0.36
0.30
α'_m
0.0
0.1
0.2
0.3
0.4
0.5
0.6
0.7
0.8
0.9
$\frac{r_m}{r_0}$
$\frac{r_0}{z_0} = \sqrt{2}$

Figure 5a

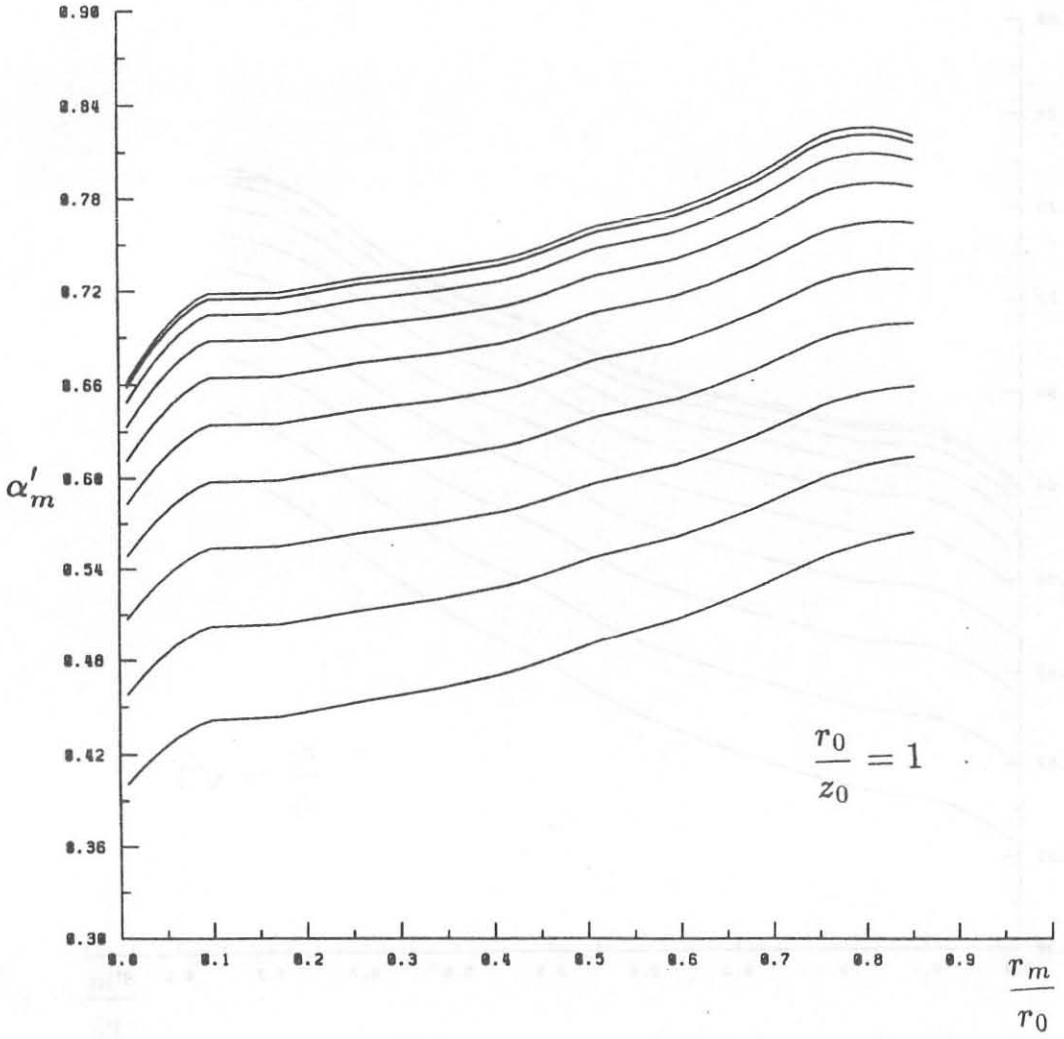
0.90
0.84
0.78
0.72
0.66
0.60
0.54
0.48
0.42
0.36
0.30
α'_m
0.0
0.1
0.2
0.3
0.4
0.5
0.6
0.7
0.8
0.9
$\frac{r_m}{r_0}$
$\frac{r_0}{z_0} = 1$

Figure 5b

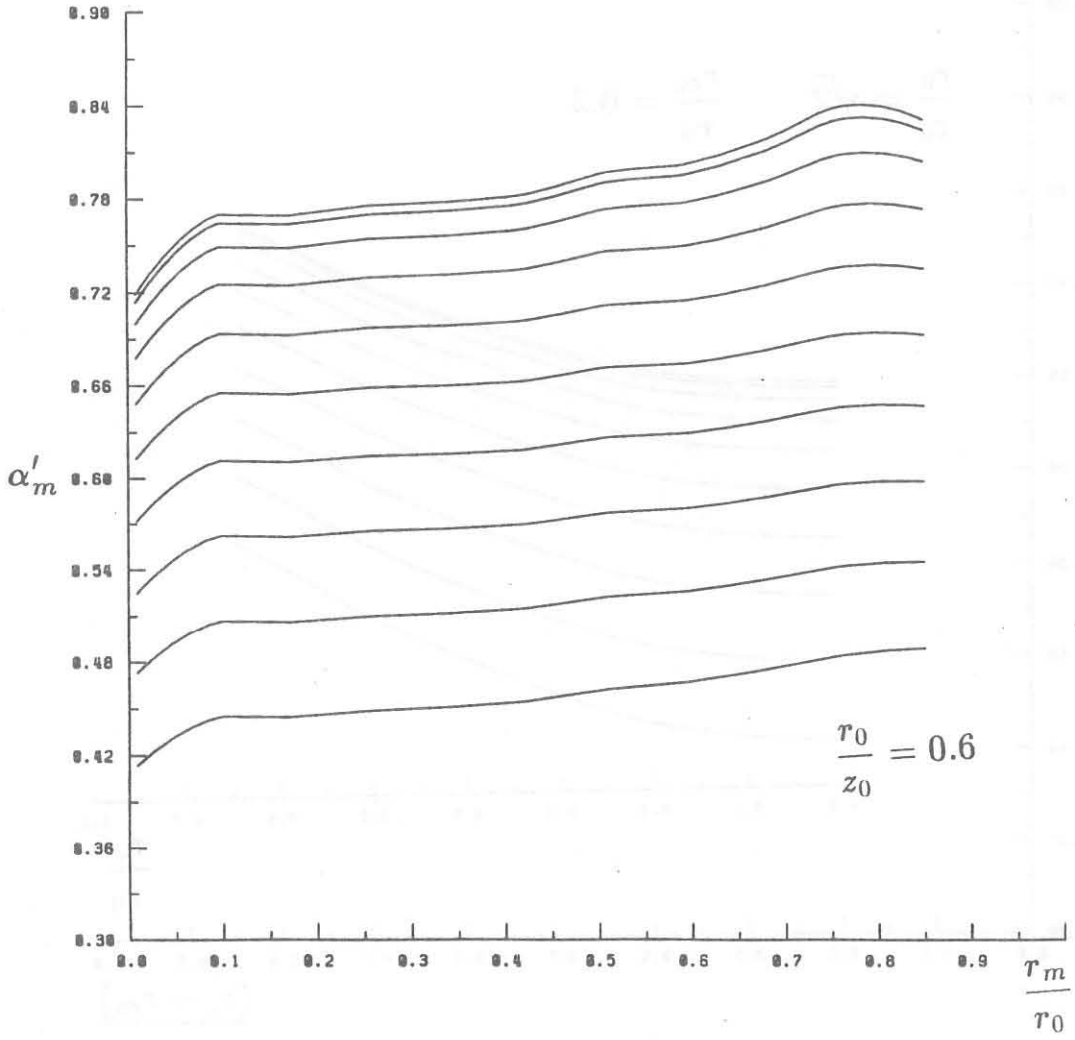
0.90
0.84
0.78
0.72
0.66
0.60
0.54
0.48
0.42
0.36
0.30
α'_m
0.0
0.1
0.2
0.3
0.4
0.5
0.6
0.7
0.8
0.9
$\frac{r_m}{r_0}$
$\frac{r_0}{z_0} = 0.6$

Figure 5c

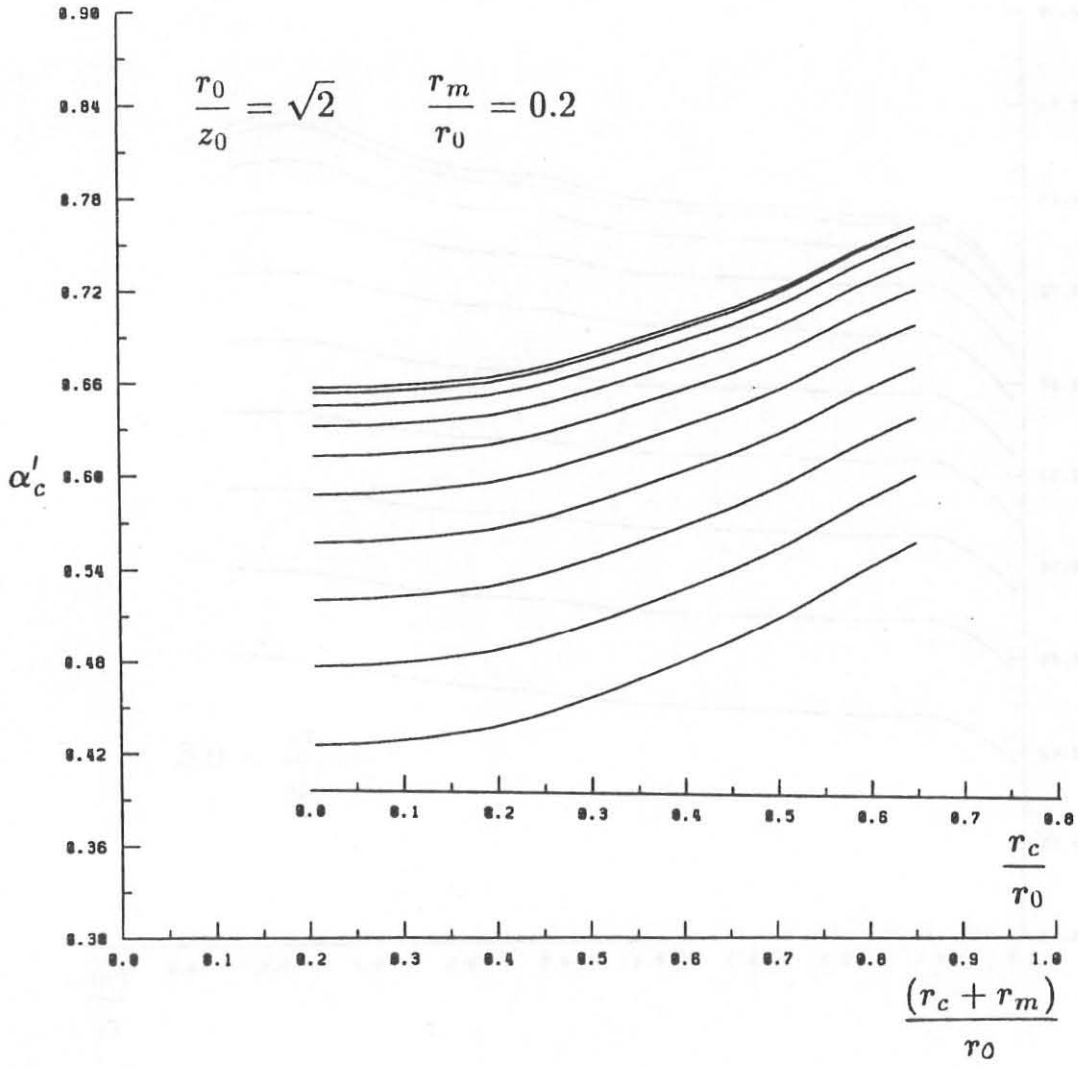
$\frac{r_0}{z_0} = \sqrt{2}$
$\frac{r_m}{r_0} = 0.2$
α_c'
0.90
0.84
0.78
0.72
0.66
0.60
0.54
0.48
0.42
0.36
0.30
0.0
0.1
0.2
0.3
0.4
0.5
0.6
0.7
0.8
0.9
1.0
$\frac{r_c}{r_0}$
$\frac{(r_c + r_m)}{r_0}$

Figure 6a

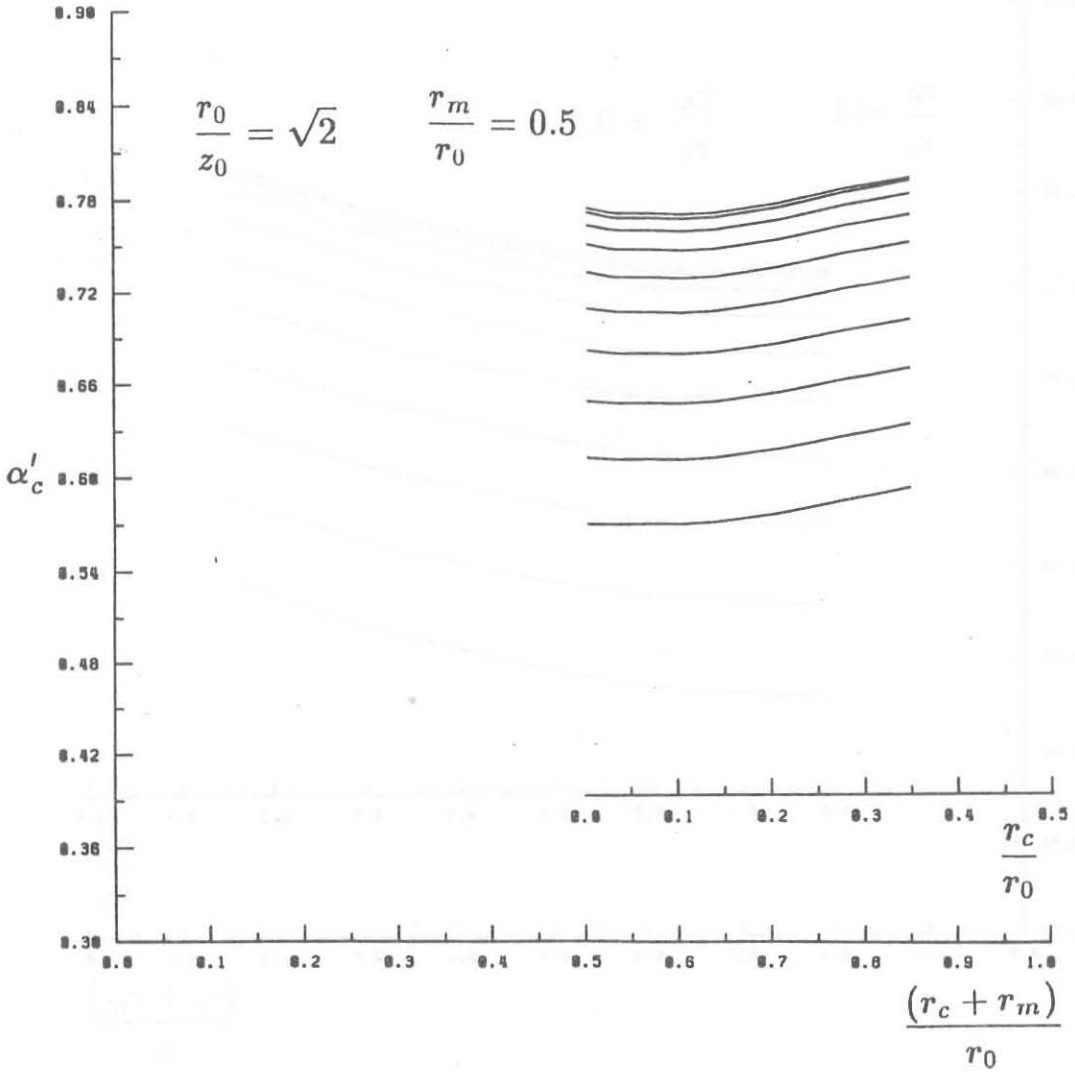
$\frac{r_0}{z_0} = \sqrt{2}$
$\frac{r_m}{r_0} = 0.5$
α_c'
0.90
0.84
0.78
0.72
0.66
0.60
0.54
0.48
0.42
0.36
0.30
0.0
0.1
0.2
0.3
0.4
0.5
0.6
0.7
0.8
0.9
1.0
$\frac{(r_c + r_m)}{r_0}$
$\frac{r_c}{r_0}$

Figure 6b

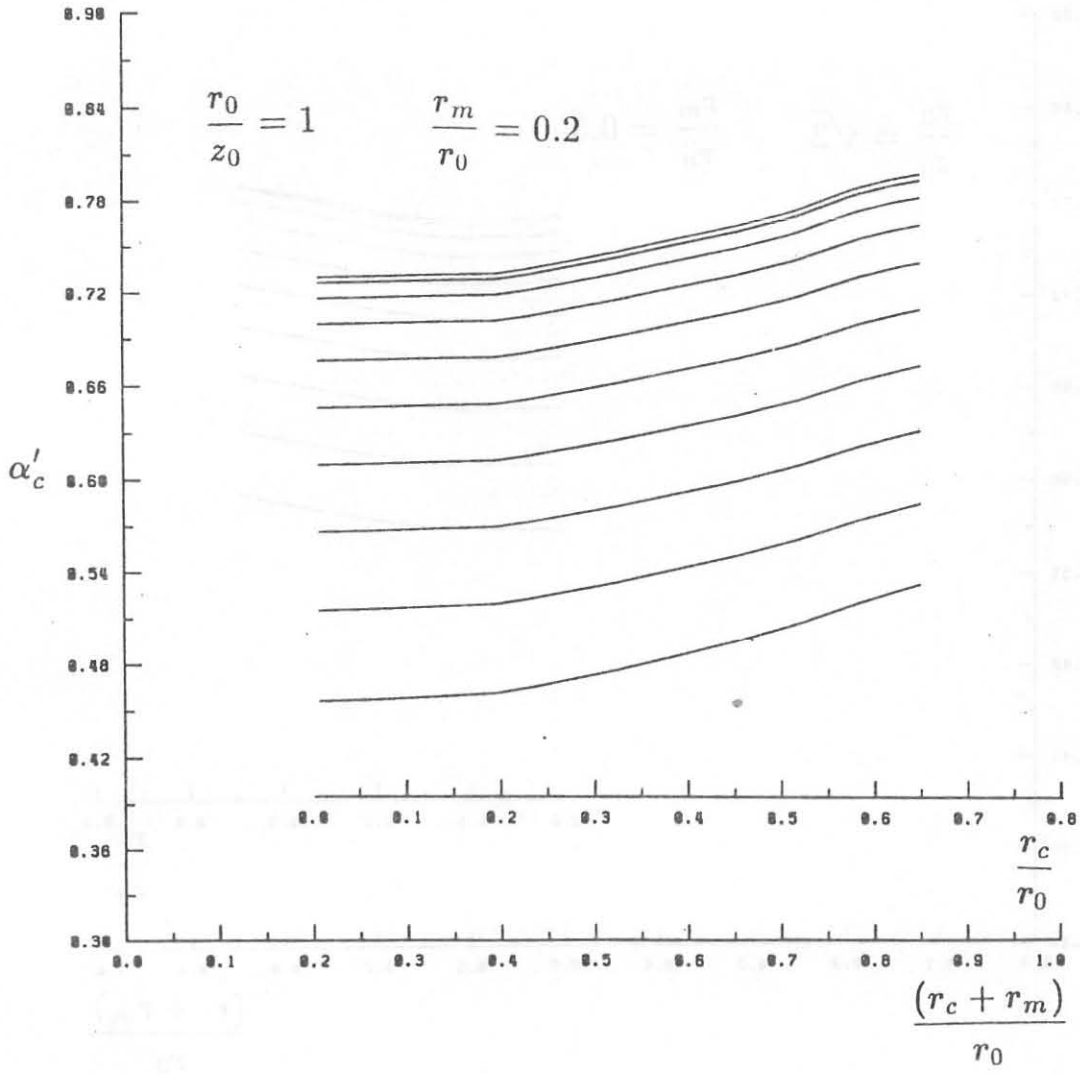
$\frac{r_0}{z_0} = 1$
$\frac{r_m}{r_0} = 0.2$
α_c'
0.90
0.84
0.78
0.72
0.66
0.60
0.54
0.48
0.42
0.36
0.30
0.0
0.1
0.2
0.3
0.4
0.5
0.6
0.7
0.8
$\frac{r_c}{r_0}$
0.0
0.1
0.2
0.3
0.4
0.5
0.6
0.7
0.8
0.9
1.0
$\frac{(r_c + r_m)}{r_0}$

Figure 7a

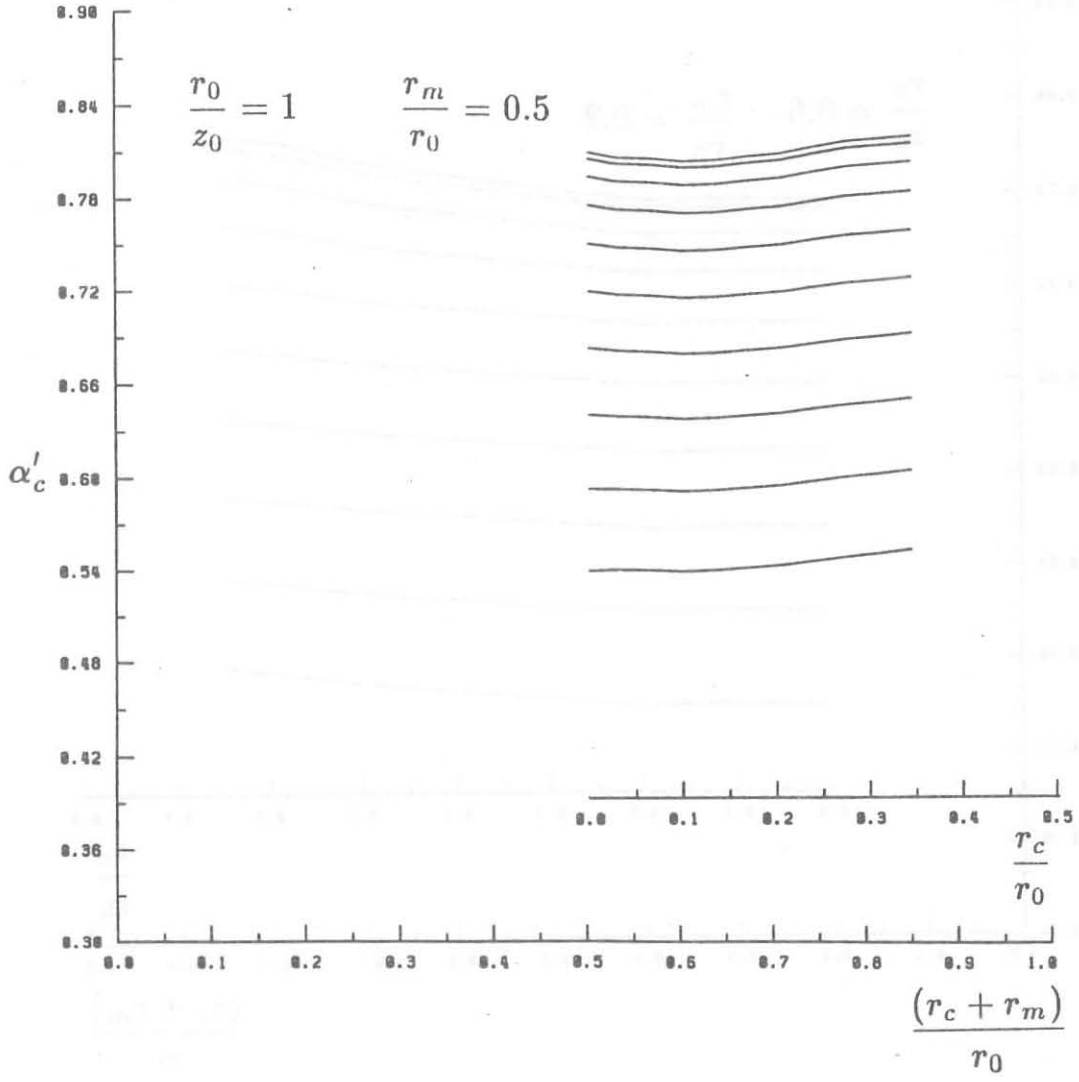
$\frac{r_0}{z_0} = 1$
$\frac{r_m}{r_0} = 0.5$
α_c'
0.90
0.84
0.78
0.72
0.66
0.60
0.54
0.48
0.42
0.36
0.30
0.0
0.1
0.2
0.3
0.4
0.5
0.6
0.7
0.8
0.9
1.0
$\frac{r_c}{r_0}$
$\frac{(r_c + r_m)}{r_0}$

Figure 7b

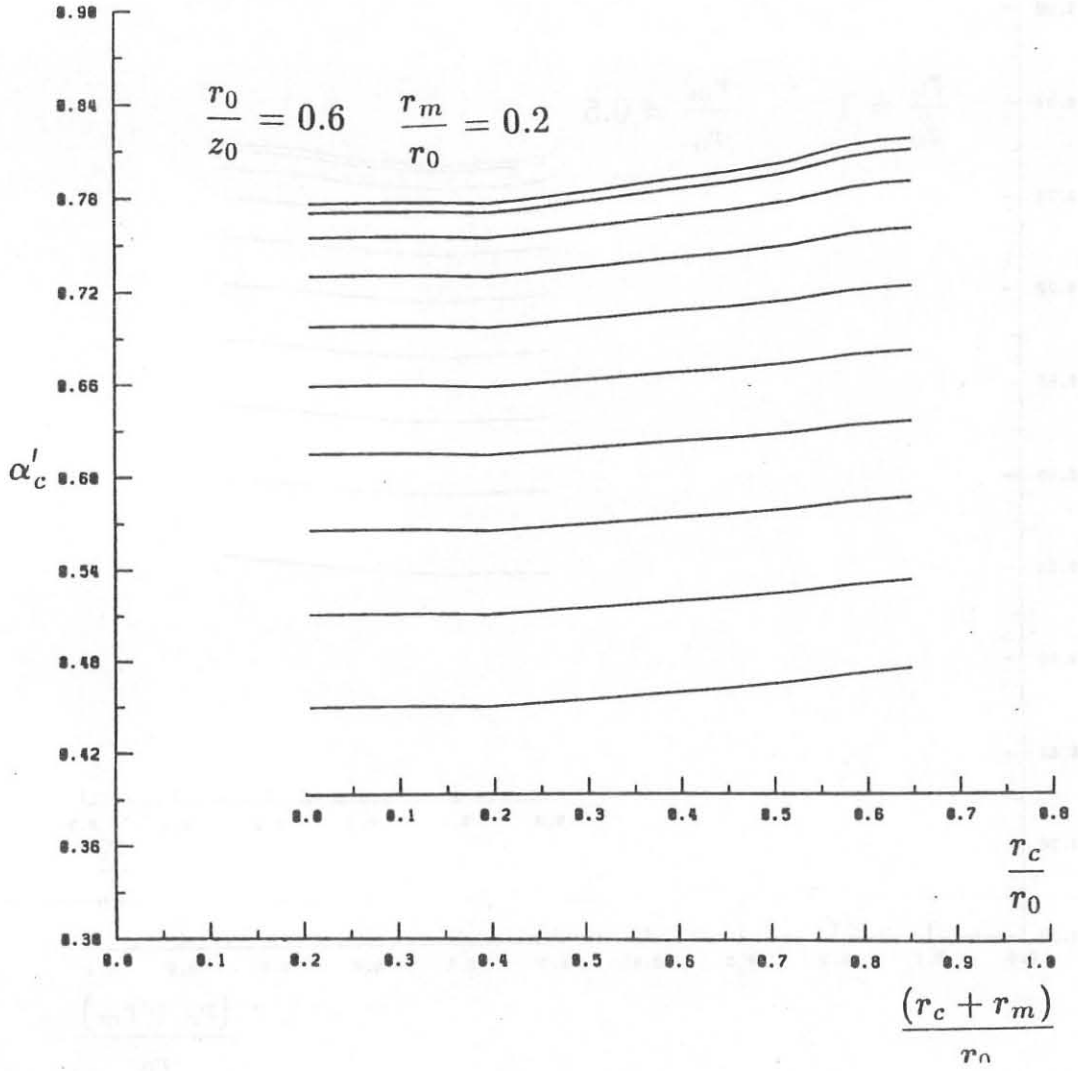
$\frac{r_0}{z_0} = 0.6$
$\frac{r_m}{r_0} = 0.2$
α'_c
0.90
0.84
0.78
0.72
0.66
0.60
0.54
0.48
0.42
0.36
0.30
0.0
0.1
0.2
0.3
0.4
0.5
0.6
0.7
0.8
0.9
1.0
$\frac{r_c}{r_0}$
$\frac{(r_c + r_m)}{r_0}$

Figure 8a

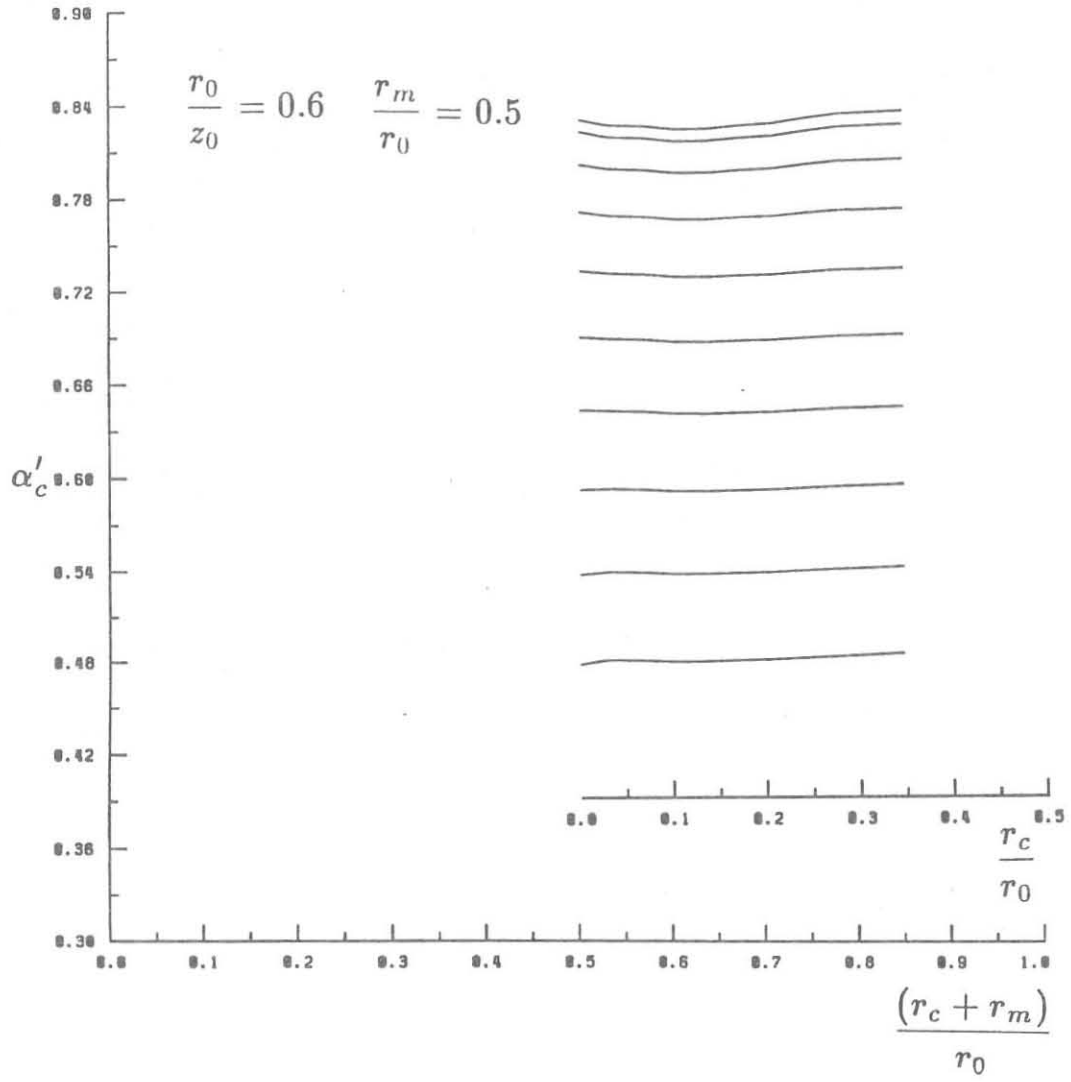
$\frac{r_0}{z_0} = 0.6$
$\frac{r_m}{r_0} = 0.5$
α'_c
0.90
0.84
0.78
0.72
0.66
0.60
0.54
0.48
0.42
0.36
0.30
0.0
0.1
0.2
0.3
0.4
0.5
0.6
0.7
0.8
0.9
1.0
$\frac{r_c}{r_0}$
$\frac{(r_c + r_m)}{r_0}$

Figure 8b